Isospin-induced effects in hot deformed $A \approx 90$ nuclei

N. Arunachalam, A. Mohamed Akbar, S. Veeraraghavan,* and M. Rajasekaran[†]

Department of Physics, Government Arts College, Tiruvannamalai 606 603, India

Isospin fluctuations and triaxial deformation are incorporated in the statistical theory of hot nuclei, and various nuclear parameters are extracted as functions of isospin, temperature, and deformation for nuclei around Zr. Shape changes are observed with changes in isospin and temperature. Above a particular temperature the shape is found to remain unchanged for all isospins. Constant entropy lines are drawn and yrast traps are observed. The yrast traps at the low entropy values indicate the neutron-proton shell closure for the systems considered. A shift in the yrast minima towards lower isospin is predicted with increase in entropy. At higher entropy values yrast minima are found to disappear. The neutron-proton asymmetry parameter calculated for $A = 90$, 92, 94, and 96 is found to depend strongly on deformation and isospin at low temperatures. For all these nuclei the asymmetry parameter is found to be a maximum for isospins corresponding to stable neutron-proton combination. The single-particle level-density parameter for $A = 90$ extracted as a function of temperature for various isospins shows a minimum at a total isospin of $\tau = 5$, indicating the higher stability of this isospin state. At higher temperatures the empirical value of $a \approx A/10$ is reproduced.

I. INTRODUCTION

Heisenberg [1] and Wigner and Feenberg [2] treated neutrons and protons as nucleons in two different isospin states and extracted many nuclear properties. Rajasekaran *et al.* [3] studied the effect of shell structure on isospin multiplets and extracted the neutron-proton asymmetry parameter as a function of temperature, biaxial deformation, and isospin.

In this work the earlier calculations [3–16] have been extended to include triaxial deformation into the picture and calculations are performed for the nuclei around Zr. The reason for choosing nuclei around ^{90}Zr is that experiments [17] in which Zr is formed as a fused-compound system in reactions such as ^{58}Ni(^{29}Si,$2pn$)^{84}Zr have been recently reported. The present work brings out the following important points.

(1) The neutron-proton asymmetry parameter is strongly dependent on the shell structure, which is grossly different for various deformation of the nucleus. In fact, there is a strong possibility for the nuclei to be triaxially deformed, and this fact is given importance in this work.

(2) The asymmetry energy contributions are found to be less significant at large temperatures because of the fluctuations in the occupation probabilities of the different single-particle states with a consequent decrease in the neutron-proton asymmetry parameter at these temperatures. The dependence of the asymmetry parameter on deformation is very strong at low temperatures. The value of this parameter is approximately equal to 19 MeV

---

*Present address: Department of Physics, Sacred Heart College, Tirupattur 635 601, India.

†Present address: Department of Nuclear Physics, University of Madras, Guindy Campus, Madras, India.

at a temperature of 0.4 MeV and is about 8 MeV for a temperature of 1.2 MeV.

(3) The shape of the nuclei shows a strong dependence on the isospin at low temperatures and remains unaffected by isospin at higher temperatures.

(4) The single-particle level-density parameter is found to approach a constant value almost equal to the empirical value $A/10$ [18,19] at high temperatures, irrespective of the isospin.

II. METHOD

A. Triaxially deformed Nilsson oscillator potential

For rotating nuclei it has been assumed that the nucleons move in a triaxially deformed Nilsson harmonic-oscillator potential with the deformation described by δ and θ. The triaxial Nilsson Hamiltonian is

$$H = p^2/2m + (m/2)(\omega_x^2 x^2 + \omega_y^2 y^2 + \omega_z^2 z^2)$$
$$+ Cl \cdot s + D(l^2 - 2\langle l^2 \rangle) . \tag{1}$$

The three oscillator frequencies are given by

$$\omega_x = \omega_0[1 - (2\delta/3)\cos(\theta - 2\pi/3)] ,$$
$$\omega_y = \omega_0[1 - (2\delta/3)\cos(\theta + 2\pi/3)] , \tag{2}$$
$$\omega_z = \omega_0[1 - (2\delta/3)\cos\theta] ,$$

with the constraint that the total volume remains constant such that

$$\omega_x \omega_y \omega_z = \mathring{\omega}_0^3 = \text{const} .$$

The deformation parameters δ and θ are varied in the range $\delta = 0.0$–0.6 with $\Delta\delta = 0.1$ and $\theta = -180°$ to $-120°$ with $\Delta\theta = 20°$. For the Nilsson parameters κ, μ and for $\hbar\mathring{\omega}_0$ the following values [20] are chosen:

$\kappa = 0.093$,

$\mu = 0.15$, $\qquad\qquad\qquad$ (3)

$\hbar\omega_0 = 45.3$ MeV$/(A^{1/3} + 0.77)$.

The single-particle levels generated with the above parameters are used for the nucleons since protons and neutrons are treated as nucleons in two different isospin states. The triaxial Nilsson Hamiltonian is diagonalized [21] in the cylindrical representation [22] using the matrix elements given in Ref. [23]. The triaxially deformed single-particle Nilsson levels are generated for $N = 5$ and the number of levels is found to be sufficient for the range of temperatures used in our calculations. The necessity of renormalizing the total energy does not arise here, since we are interested only in the energy differences between the excited and ground states of the system and not in the actual magnitude of the energies.

B. Statistical theory

In the statistical formalism, we start with the grand canonical partition function $Q_0(\alpha,\beta,\gamma)$ for a system of A nucleons at a temperature $T = 1/\beta$. The Lagrangian multipliers α, β, and γ conserve the total number of particles, total energy, and total isospin of the system [24,25]:

$$Q_0(\alpha,\beta,\gamma) = \sum_{E_i,N_i,\tau_i} \exp(\alpha N_i - \beta E_i + \gamma\tau_i) . \qquad (4)$$

The partition function in Eq. (4) does not include the Coulomb interaction, which will be added subsequently. The average number of particles, average total energy, and z component of the total isospin are projected out of the partition function by the following equations:

$$\langle N \rangle = A = \frac{\partial \ln Q_0}{\partial\alpha} , \qquad (5)$$

$$\langle E \rangle = -\frac{\partial \ln Q_0}{\partial\beta} , \qquad (6)$$

$$\langle \tau \rangle = \frac{\partial \ln Q_0}{\partial\gamma} . \qquad (7)$$

The corresponding equations in terms of the single-particle energies ε_i are

$$\langle N \rangle = A = \sum n_i^+ + \sum n_i^- , \qquad (8)$$

$$\langle E \rangle = \sum (n_i^+ + n_i^-)\varepsilon_i , \qquad (9)$$

$$\langle \tau \rangle = \sum n_i^+ \tau_z^+ + \sum n_i^- \tau_z^- , \qquad (10)$$

where n_i^+ and n_i^- are the occupation probabilities at single-particle energies ε_i of neutrons and protons with isospin projections $\tau_z^+ = +\frac{1}{2}$ and $\tau_z^- = -\frac{1}{2}$, respectively,

$$n_i^+ = [1 + \exp(-\alpha + \beta\varepsilon_i + \gamma\tau_z^+)]^{-1} ,$$
$$n_i^- = [1 + \exp(-\alpha + \beta\varepsilon_i + \gamma\tau_z^-)]^{-1} . \qquad (11)$$

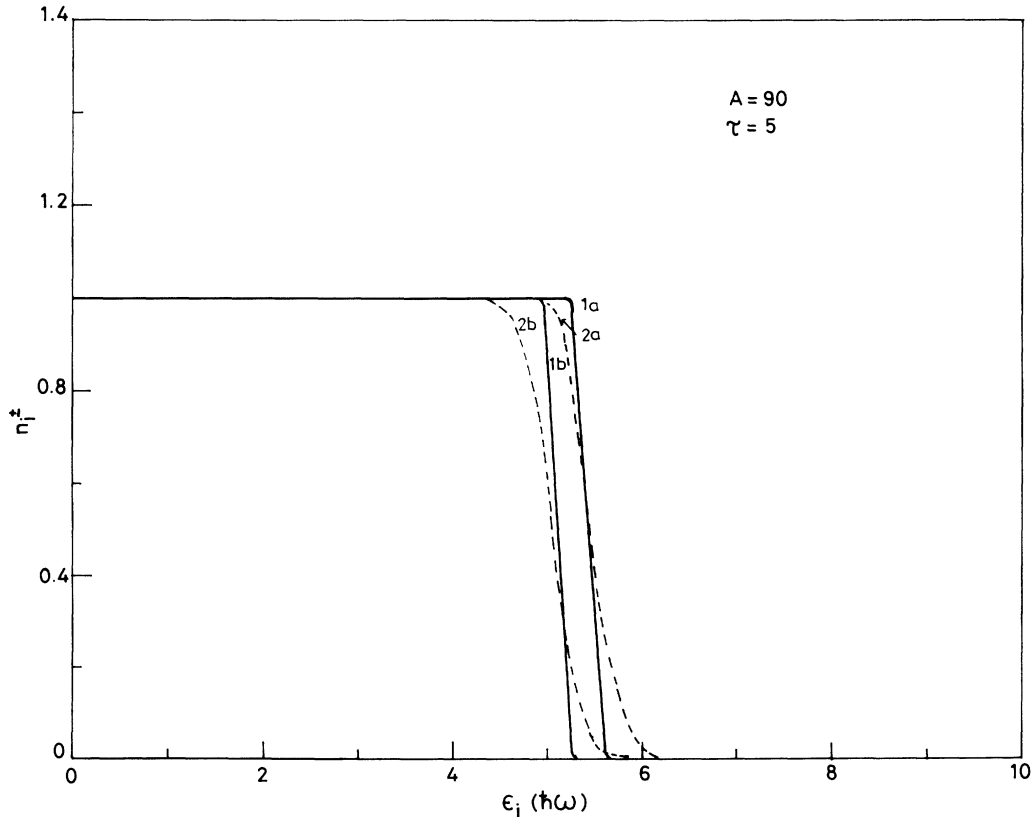The occupation probabilities are displayed in Fig. 1 as a

FIG. 1. Occupation probabilities n_i^+ (1a and 2a) for τ_z^+ and n_i^- (1b and 2b) for τ_z^- as a function of the single-particle energies for $A = 90$ corresponding to a total isospin of 5. The solid curves are for $T = 0.3$ MeV, whereas the dashed curves are for $T = 1.2$ MeV.

function of ε_i for the two states $\tau_z^{\pm}$.

The coupled nonlinear equations (8) and (10) have to be solved for the Lagrangian multipliers α and β for a given mass number A, temperature T, and z component of the total isospin τ [$=(N-Z)/2$] of the system. The energy of the system is then calculated using Eq. (9). The corresponding excitation energy $E^*(\tau, T, \delta, \theta)$ and the entropy $S(\tau, E^*, \delta, \theta)$ are obtained using the following expressions:

$$E^*(\tau, T, \delta, \theta) = \sum (n_i^+ + n_i^-)\varepsilon_i - \sum_{i=1}^{A} \varepsilon_i \ ,$$

$$S(\tau, E^*, \delta, \theta) = S^+ + S^- \ , \tag{12}$$

where

$$S^+ = -\sum [n_i^+ \ln n_i^+ + (1 - n_i^+)\ln(1 - n_i^+)] \ ,$$

$$S^- = -\sum [n_i^- \ln n_i^- + (1 - n_i^-)\ln(1 - n_i^-)] \ . \tag{13}$$

The level densities for various excitation energies and isospins of the system are given by

$$\rho(\tau, E^*, \delta, \theta) = \beta \exp[S(\tau, E^*, \delta, \theta)] / S_{max} \ . \tag{14}$$

The normalization factor S_{max} depends upon the dimensionality of phase space, which is the number of eigenstates used [14].

The total energy E of the system for each temperature T is minimized with respect to the deformation parameters δ and θ. The lines of constant entropy are then drawn in the E^*-vs-τ plane for $A = 90$, 92, 94, and 96 (the results are displayed in Figs. 6–9). Collective deexcitations along the constant entropy lines are possible through the emission of beta particles.

C. Neutron-proton asymmetry parameter

The neutron-proton asymmetry parameter a_{asy} is extracted using the approach given in Ref. [3]. In terms of the isospin τ, the variation of the binding energy with isospin is given by

$$\left[\frac{\partial B}{\partial \tau}\right]_{LDM} = -\frac{\partial M}{\partial \tau}$$

$$= -(M_n - M_p) - 8a_{asy}\tau / A - 2a_c\tau / A^{1/3}$$

$$+ a_c(A - 1)/A^{1/3} \ . \tag{15}$$

The corresponding expression in the statistical theory can be obtained using the partition function method as

$$\left[\frac{\partial B}{\partial \tau}\right]_{shell} = -\frac{\partial \Omega}{\partial \tau}$$

$$= -T\tau \left[\sum n_i^+ (1 - n_i^+)\tau_z^{+2}\right.$$

$$\left. + \sum n_i^- (1 - n_i^-)\tau_z^{-2}\right]^{-1}$$

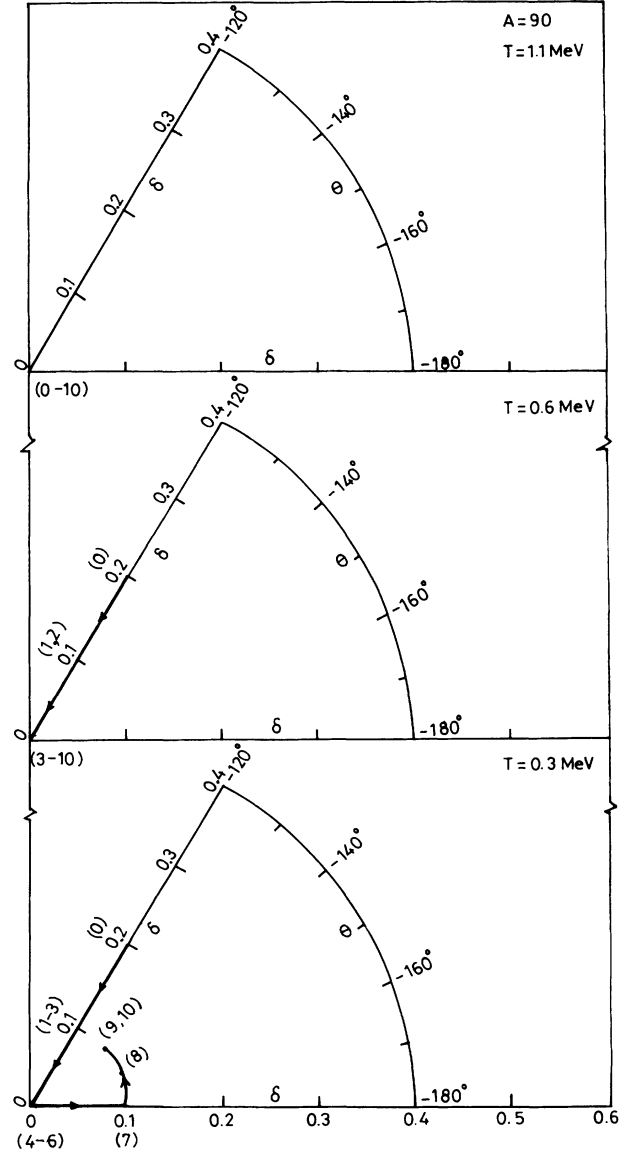$$-2a_c\tau / A^{1/3} + a_c(A - 1)/A^{1/3} \ , \tag{16}$$

FIG. 2. Isospin trajectory in the δ-θ plane showing the calculated minimum-energy shape as a function of isospin for $A = 90$, at different temperatures. The convention used in shape parametrization is as follows: For $\theta = -180°$ the shape is oblate with the nucleus rotating around the symmetry axis; for $\theta = -120°$ the shape is prolate with the nucleus rotating around the perpendicular axis; and for other values, the nucleus is triaxial.

where the thermodynamical potential Ω (free energy), which is the negative of the binding energy, is related to the partition function as

$$Q = \exp(-\beta\Omega) \ . \tag{17}$$

The first term on the right-hand side of Eq. (16) has been obtained from the partition function as

$$\frac{\partial(T \ln Q_0)}{\partial \tau} = T\left[\frac{\partial \ln Q_0}{\partial \gamma}\right]\frac{\partial \gamma}{\partial \tau} \ . \tag{18}$$

Equation (16) gives the variation of the binding energy of the system with the isospin τ and can be identified with the liquid-drop-model neutron-proton asymmetry term $8a_{asy}\tau/A$. The first differential on the right-hand side is the net isospin, as can be seen from Eq. (7). Using Eqs. (5)–(11), we have

$$\frac{\partial \gamma}{\partial \tau} = - \left[\sum n_i^+ (1-n_i^+)\tau_z^{+2} + \sum n_i^- (1-n_i^-)\tau_z^{-2} \right] .$$

(19)

The other terms which are due to the classical Coulomb energy of the nucleus are the same as in the liquid-drop model. From Eqs. (15) and (16), the neutron-proton

asymmetry parameter is calculated by minimizing the total energy of the system for each temperature with respect to the deformation parameters δ and θ. Calculations are performed for $A = 90, 92, 94,$ and 96 (the results are displayed in Figs. 10–13).

D. Single-particle level-density parameter

For the calculation of the single-particle level-density parameter, the formulation of the shell correction method of Ramamurthy, Kapoor, and Kataria [13] for estimating the excitation energies of the system with respect to the ground-state energies of the shell model is adopted. The excitation energy E^* of the system is ob-
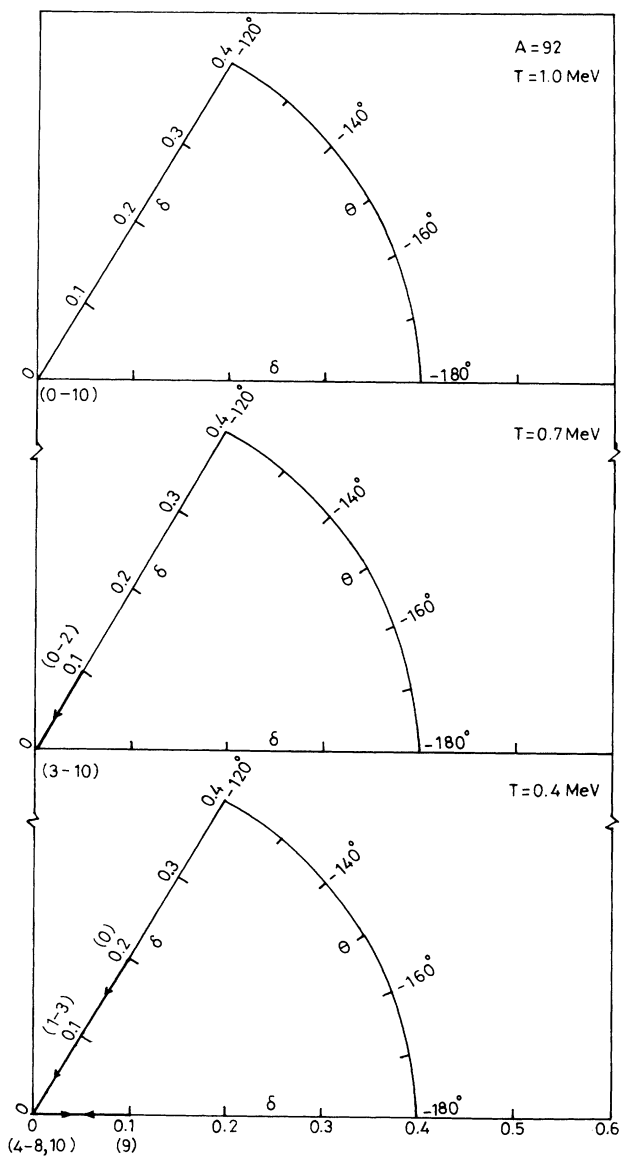

FIG. 3. Isospin trajectory in the δ-θ plane showing the calculated minimum-energy shape as a function of isospin for $A = 92$, at different temperatures.
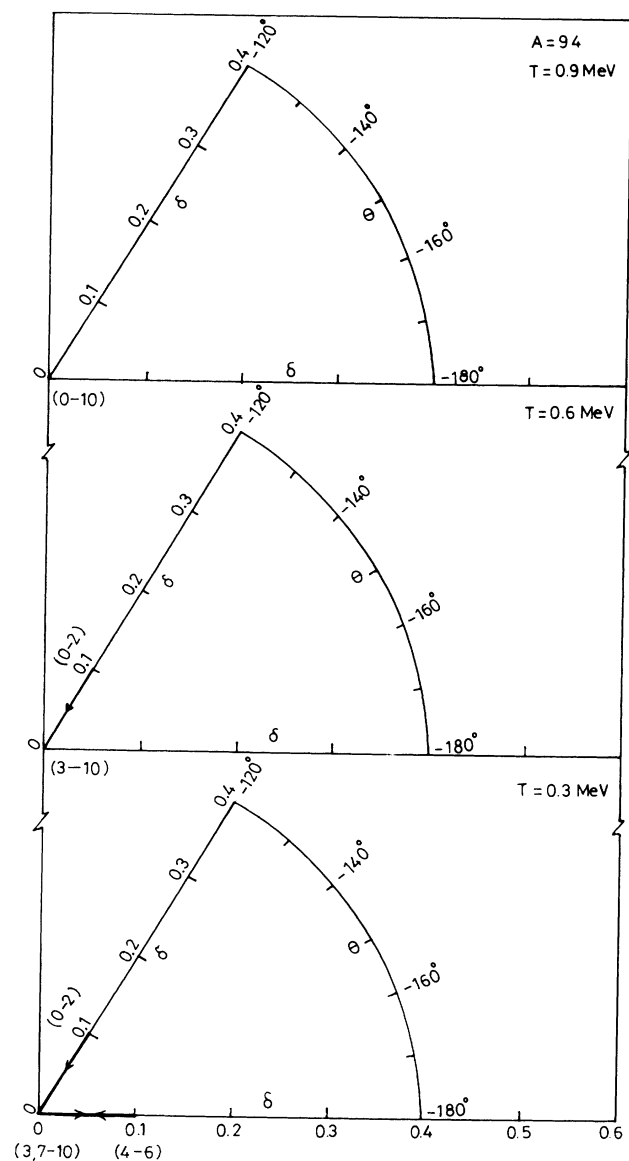
FIG. 4. Isospin trajectory in the δ-θ plane showing the calculated minimum-energy shape as a function of isospin for $A = 94$, at different temperatures.

tained using the equation

$$E^*(\tau,T,\delta,\theta)=E(\tau,T,\delta,\theta)-E_0 , \tag{20}$$

where E_0 is the ground-state energy of the nucleus. The single-particle level-density parameter $a(\tau,T,\delta,\theta)$ as a function of isospin τ, temperature T, and deformation parameters δ and θ is extracted using the equation

$$a(\tau,T,\delta,\theta)=S^2(\tau,E^*,\delta,\theta)/4E^*(\tau,T,\delta,\theta) . \tag{21}$$

Calculations are performed for $A=90$ (the results are displayed in Fig. 16).

FIG. 5. Isospin trajectory in the δ-θ plane showing the calculated minimum-energy shape as a function of isospin for $A=96$, at different temperatures.

III. RESULTS AND DISCUSSION

The occupation probabilities n_i^+ and n_i^- for the positive and negative projections of the single-particle isospin states in each single-particle level ε_i are different as the degeneracy of the isospin states is removed because of rotation in the isospin space. This is evident from Fig. 1, where these occupation probabilities are shown as a function of ε_i at low and high temperatures. Curves 1a for n_i^+ and 1b for n_i^- correspond to a total isospin $\tau=5$ at a temperature of 0.3 MeV for $A=90$. Curves 2a and 2b correspond to a temperature of 1.2 MeV for the same isospin of the system. It is evident that for a cold nuclear system the occupation probability is unity up to the Fermi level, and thereafter it is zero. With increase in temperature the occupation probabilities decrease for the levels below the Fermi energy and increase for the levels above the Fermi energy. These curves help in understanding the way of generating the net isospin of the system which can be obtained from the graph as

$$\tau= \int dn_i^+ \tau_z^+ + \int dn_i^- \tau_z^- . \tag{22}$$

The effect of temperature and isospin on the shape of nuclei was not studied hitherto in detail. The aim of this work is to study the combined effects of these two param-
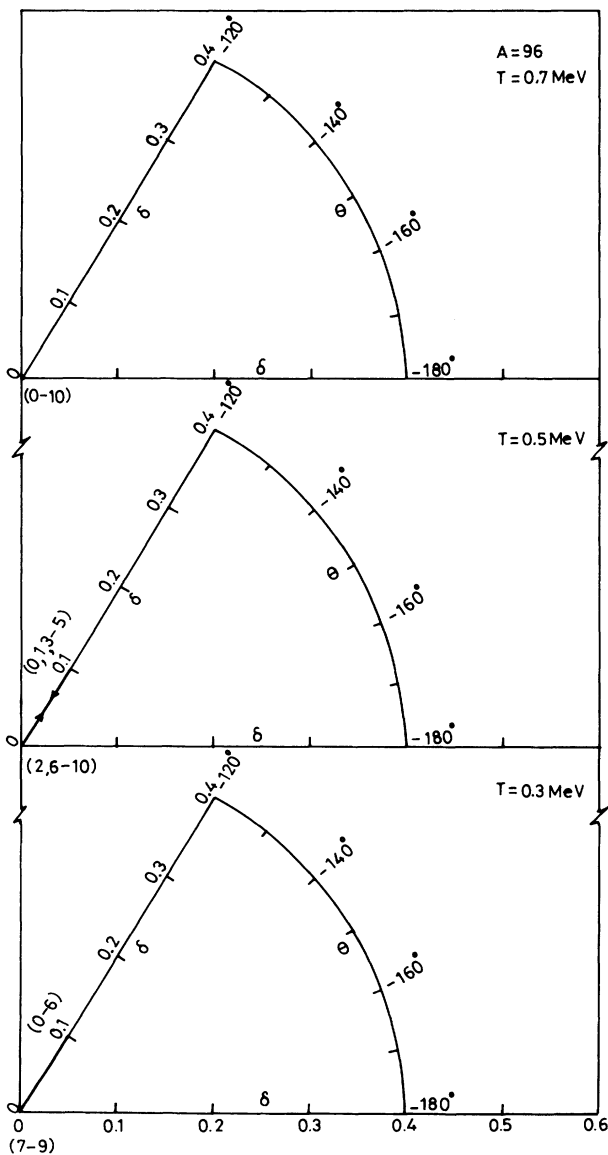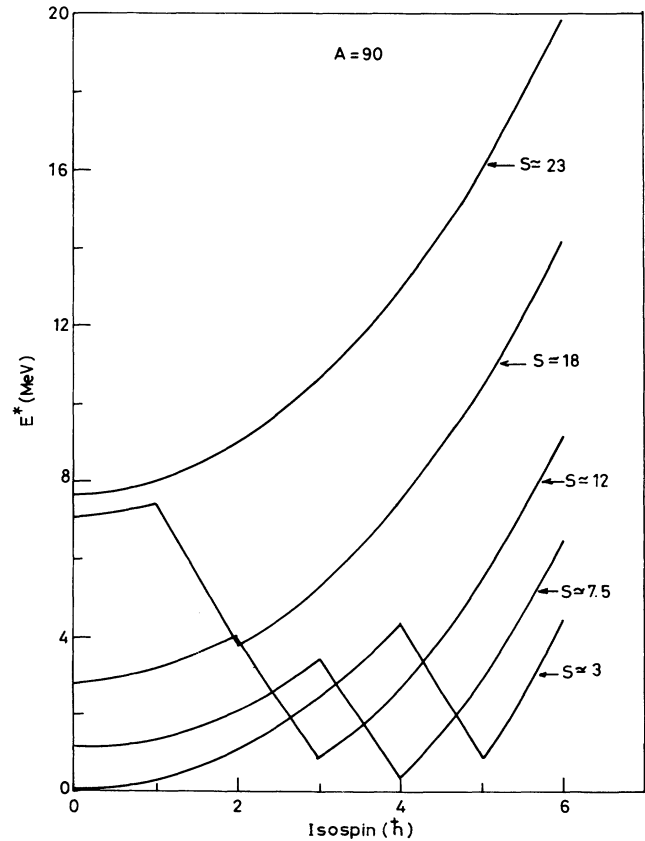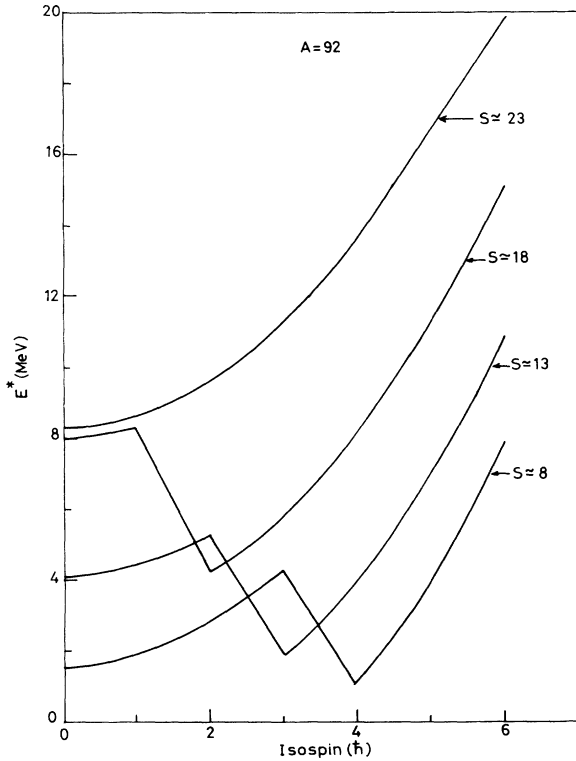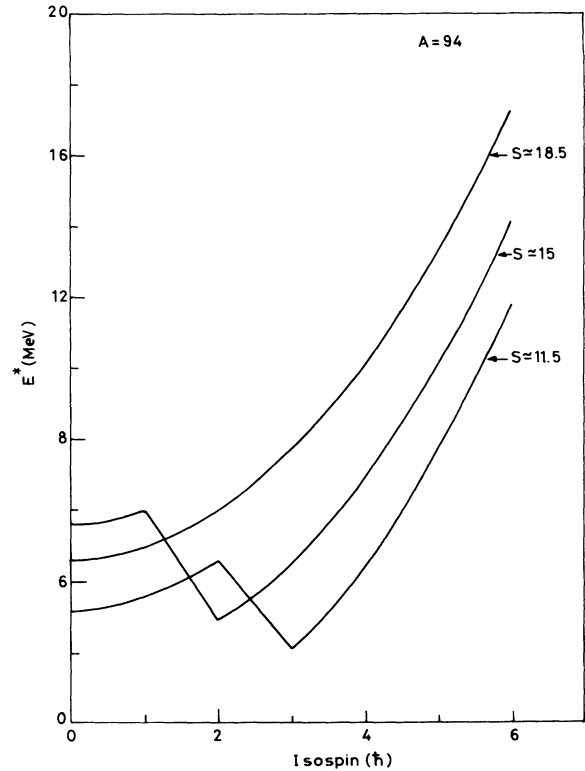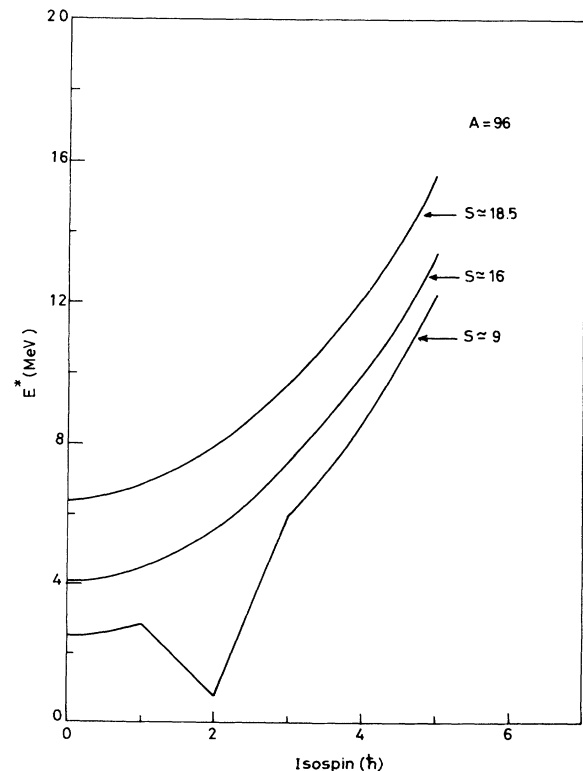

FIG. 6. Constant entropy lines for $A=90$.

FIG. 7. Constant entropy lines for $A = 92$.

FIG. 8. Constant entropy lines for $A = 94$.

eters on the shape of nuclei in the neighborhood of Zr. The hodographs of the deepest energy minimum of Zr as functions of total isospin τ and deformation parameters δ and θ, calculated at different temperatures, are shown in Figs. 2–5. From Fig. 2, for $A = 90$, we find that the nucleus is prolate for isospins from 0 to 3, spherical for isospins from 4 to 6, oblate for isospin 7, and it tries to achieve a prolate shape at higher isospins. These deformation fluctuations vanish at a high temperature of about $T = 1.1$ MeV, because of the vanishing isospin and shell effects at this temperature. From Fig. 3, for $A = 92$, we note that at $T = 0.4$ MeV the shape is prolate for initial isospins, becomes spherical for further isospins, changes to oblate for isospin 9, and finally becomes spherical for isospin 10. These shrinking and stretching effects in the deformation vanish at 1.0 MeV for ^{92}Zr. Similar behavior is observed for ^{94}Zr, as is evident from Fig. 4. In the case of ^{96}Zr, the shape changes from prolate for lower isospins to spherical for higher isospins, as depicted in Fig. 5. These changes in the shape of the nuclei suggest an impression that an interplay among isospin, temperature, and deformation is responsible for the observed behavior of the nuclei.

In the excitation energy versus isospin plane, constant entropy lines are drawn and displayed in Figs. 6–9. These curves are drawn after minimizing the total energy of the system with respect to deformation for each temperature. During isospin fluctuations [26], collective deexcitation along the constant entropy line may take

FIG. 9. Constant entropy lines for $A = 96$.

place and the system may be trapped in one of the isobaric states with a certain net isospin having relatively lower energies than the neighboring states. As reported in earlier calculations [3], yrast traps [26] are obtained in the isospin space. The occurrence of these traps is due to the interplay between total isospin, deformation, and temperature. In Fig. 6, for $A = 90$ at an entropy of $S = 3$, the yrast trap obtained at the isospin $\tau = 5$ corresponds to the stable neutron-proton combination of $N = 50$ and $Z = 40$. However, in the case of higher entropy lines, the yrast minima for isospin shift toward the lower side of the isospin axis. This shift in the yrast minima may be due to the decreasing influence of the isospin on the system at higher temperatures, perhaps with an increasing influence of the total angular momentum on the system, as reported earlier in the case of ^{40}Ca [15]. This is clear from the fact that at higher temperatures the rotation of the system plays a dominant role compared with the total isospin, which displaces the system from the stable configuration.

Figures 7–9 represent constant entropy lines for $A = 92$, 94, and 96, respectively. In all these cases the yrast minima at lower entropy values correspond to the neutron shell closure at $N = 50$. But at higher entropy values, the yrast minima indicate a shift from the stable configuration for $A = 92$ and 94, as in the case of $A = 90$. However, at still higher entropy values, the yrast minima are found to disappear because of vanishing shell effects.

The variation of the asymmetry parameter as a function of total isospin and temperature is depicted in Fig. 10 for $A = 90$. This parameter is obtained after minimizing the total energy of the system with respect to defor-

FIG. 11. Variation of asymmetry parameter with isospin at various temperatures in the case of $A = 96$ for minimized total energy with respect to deformation.
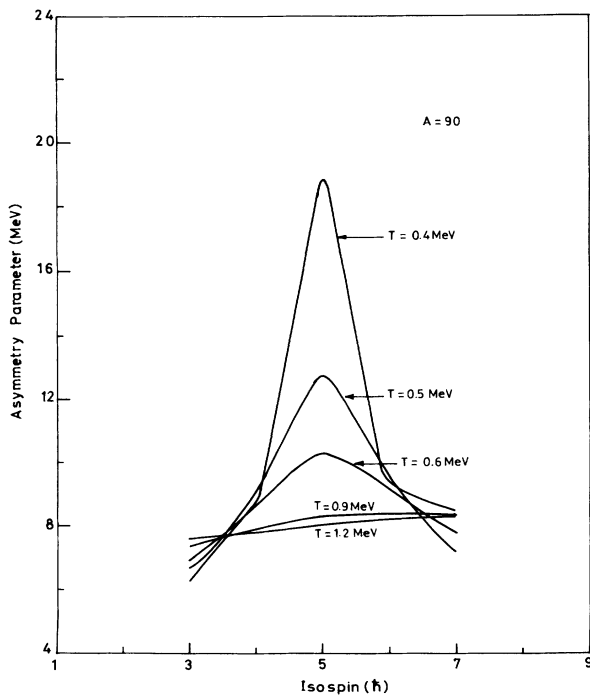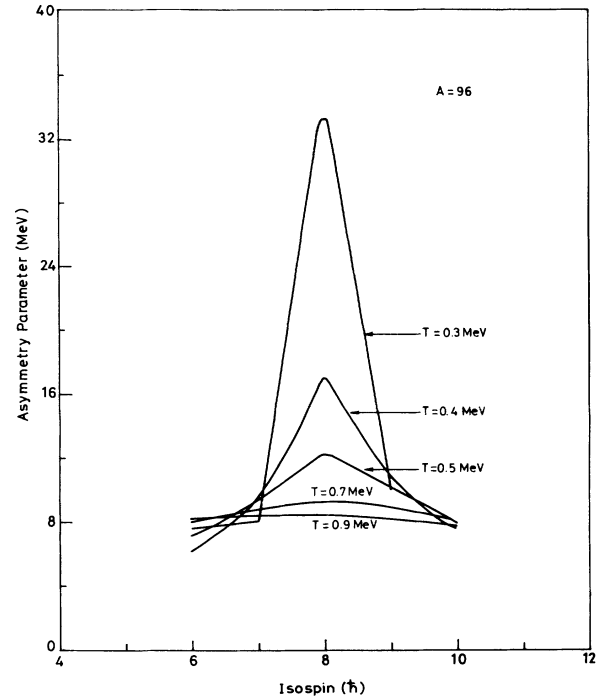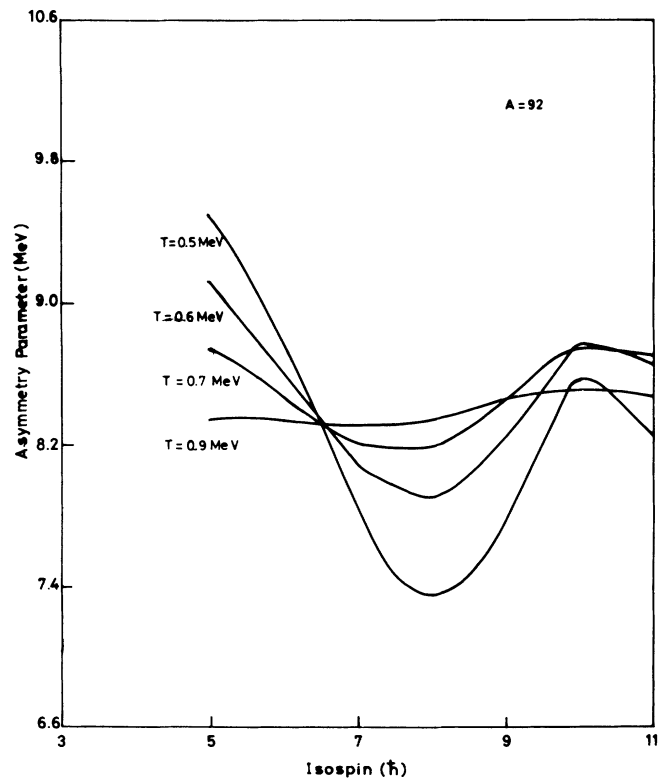

FIG. 10. Variation of asymmetry parameter with isospin at various temperatures in the case of $A = 90$ for minimized total energy with respect to deformation.

FIG. 12. Variation of asymmetry parameter with isospin at various temperatures in the case of $A = 92$ for minimized total energy with respect to deformation.

mation for each temperature. The asymmetry parameter shows a maximum at all temperatures for $\tau=5$, corresponding to the stable neutron number $N=50$ and proton number $Z=40$. It is obvious from the figure that higher temperatures cause a decrease in the maximum at the isospin $\tau=5$. Similar curves drawn for $A=96$ are shown in Fig. 11. The maxima obtained corresponding to $\tau=8$ at all temperatures indicate a subshell closure at $Z=40$ and $N=56$.

The asymmetry parameter for $A=92$ in Fig. 12 shows peaks at $\tau=10$ at all temperatures. This corresponds to a neutron subshell closure at $N=56$. At higher temperatures, the maximum value of the asymmetry parameter is reduced.

In Fig. 13, for $A=94$, the maximum value of the asymmetry parameter corresponding to the isospin $\tau=9$ at all temperatures indicates the simultaneous neutron subshell closure at $N=56$ and proton subshell closure at $Z=38$. The energy minimum for this isospin occurs for $\delta=0.0$, $\theta=-180°$, and $\omega=0.0$, corresponding to the spherical shape of the nucleus. The low-temperature curve for $T=0.3$ MeV shows an additional maximum at $\tau=7$, corresponding to the proton subshell closure at $Z=40$. From Figs. 10–13 it is evident that at higher temperatures the isospin effects are reduced in the case of ^{90,92,94,96}Zr.

Figure 14 shows the variation of the asymmetry parameter as a function of the total isospin and deformation parameter θ, for $A=90$ and 96. The asymmetry parameter is found to be strongly dependent on deformation and shows a maximum at $\tau=5$ for $A=90$ and at $\tau=8$ for $A=96$ for the temperature $T=0.4$ MeV. This indicates

FIG. 14. Variation of the asymmetry parameter with isospin for various deformations for $A=90$ and 96.
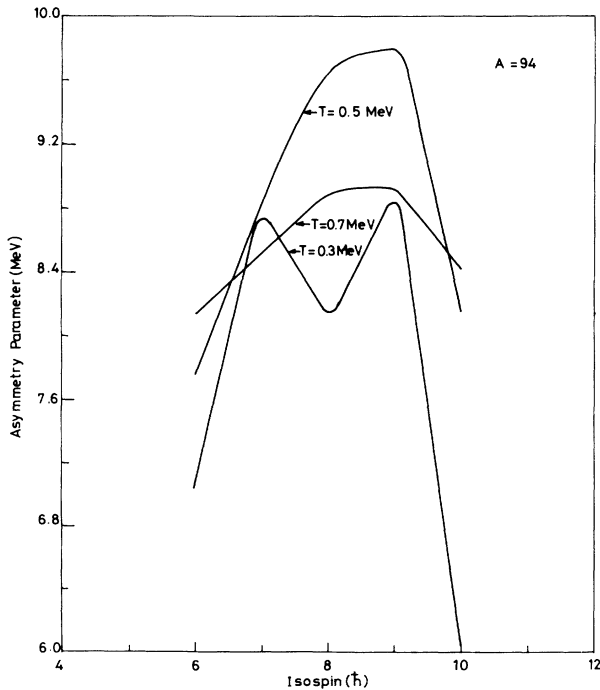

FIG. 13. Variation of asymmetry parameter with isospin at various temperatures in the case of $A=94$ for minimized total energy with respect to deformation.
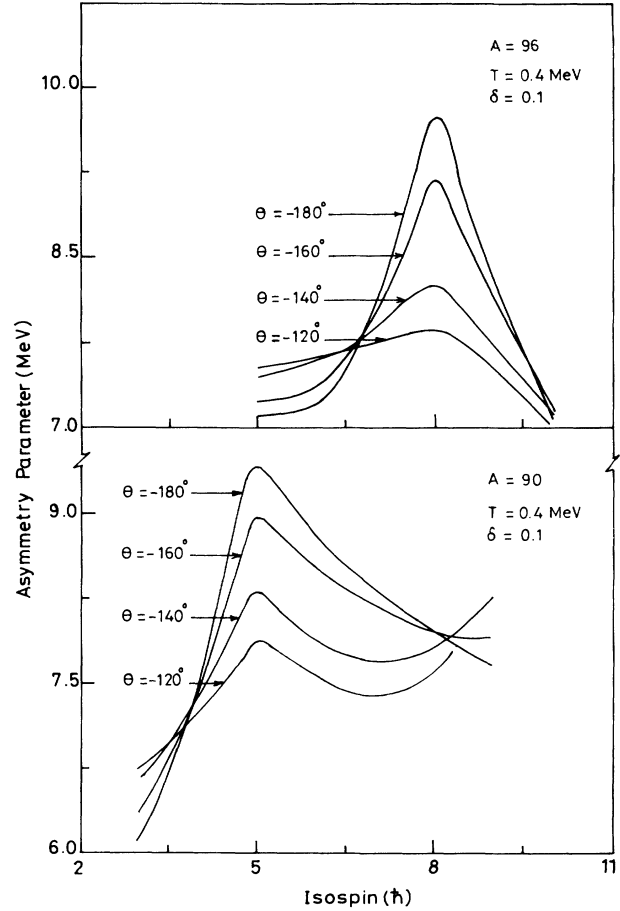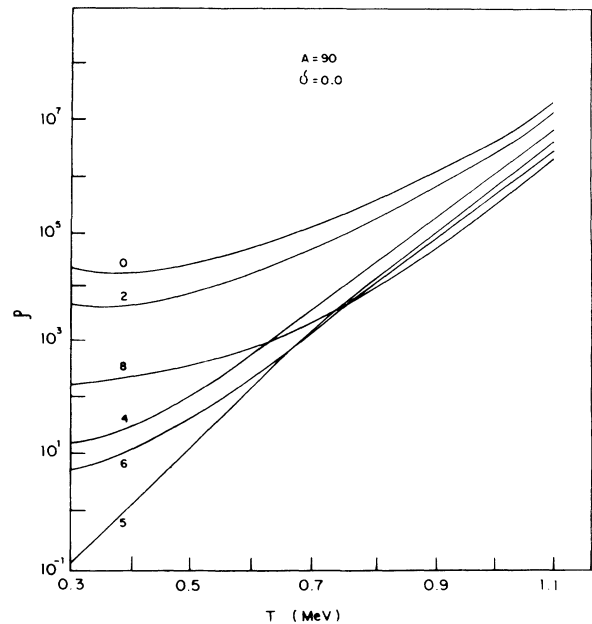

FIG. 15. Variation of level density with temperature for various isospins of the isobar $A=90$. The numbers on the curve refer to the net isospin of the system.
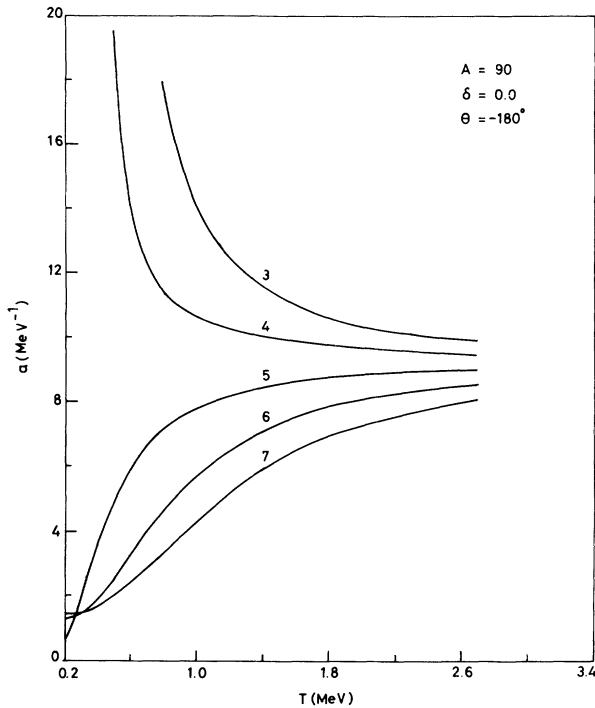
FIG. 16. Variation of the single-particle level-density parameter with temperature for various isospins of the isobar $A = 90$. The numbers on the curve refer to the net isospin of the system.

the stable configuration of $Z = 40$, $N = 50$ for $A = 90$, and $Z = 40$, $N = 56$ for $A = 96$. The maximum value of the asymmetry parameter in both cases is found to decrease as θ changes from $-180°$ to $-120°$, implying the effect of shape transition from oblate to prolate on the asymmetry energy.

Figure 15 shows the variation of level density as a function of temperature and isospin for $A = 90$. The striking feature of the graph is that the level density corresponding to the total isospin $\tau = 5$ is the lowest at reasonably low temperatures. This isospin incidentally implies the closed shells at $N = 50$ and $Z = 40$. The level density for isospins both above and below this isospin is much higher.

In Fig. 16, the variation of the single-particle level-density parameter a $(\tau, T, \delta, \theta)$ with temperature for various isospins of the isobar $A = 90$ is depicted. The level-density parameter corresponding to the isospin $\tau = 5$ is minimum at low temperatures, indicating the higher stability of this state compared with the other isospin values. At higher temperatures, however, the effect of the isospin is less significant and the curves converge to the value predicted by experimental observation, which is given by the empirical relation a $\simeq A/10$.

We conclude that the statistical theory with the inclusion of isospin, shape, and temperature degrees of freedom with the single-particle levels as the only input predicts the most stable isobar for a given A. In the results presented here, the interplay between the various degrees of freedom has been clearly brought out. However, pairing correlations and rotation of the nuclei may also be incorporated into the formalism for a complete study.

ACKNOWLEDGMENTS

[1] W. Heisenberg, Z. Phys. 77, 1 (1932).

[2] E. P. Wigner and E. Feenberg, Prog. Theor. Phys. 8, 274 (1941).

[3] M. Rajasekaran, N. Arunachalam, T. R. Rajasekaran, and V. Devanathan, Phys. Rev. C 38, 1926 (1988).

[4] M. Brack, J. Damgaard, A. S. Jensen, H. C. Pauli, V. M. Strutinsky, and C. Y. Wong, Rev. Mod. Phys. 44, 320 (1972).

[5] N. Carjan, A. Delagrange, and A. Fluery, Phys. Rev. C 19, 2267 (1979).

[6] P. A. Seeger, in Proceedings of the International Conference on the Properties of Nuclei far from the Region of Beta Stability, Switzerland, 1970 (unpublished), Vol. 1, p. 217.

[7] L. G. Moretto, Nucl. Phys. A182, 641 (1972); A185, 145 (1972); A216, 1 (1973).

[8] A. V. Ignatyuk, Sov. J. Phys. 9, 208 (1969).

[9] T. Ericson, Adv. Phys. 9, 425 (1960).

[10] O. Civitarese and A. L. Depaoli, Nucl. Phys. A440, 480 (1980).

[11] O. Civitarese, A. Plastino, and Amand Faessler, J. Phys. G 9, 1063 (1983).

[12] V. M. Strutinsky, Nucl. Phys. A95, 420 (1967).

[13] V. S. Ramamurthy, S. S. Kapoor, and S. K. Kataria, Phys. Rev. Lett. 25, 386 (1970).

[14] M. Rajasekaran and V. Devanathan, Phys. Lett. 104B, 95 (1981); 113B, 433 (1982); Phys. Rev. C 24, 2606 (1981).

[15] M. Rajasekaran, N. Arunachalam, and V. Devanathan, Phys. Rev. C 36, 1860 (1987).

[16] M. Rajasekaran, T. R. Rajasekaran, and N. Arunachalam, Phys. Rev. C 37, 307 (1988).

[17] D. J. Bluementhal, C. J. Lister, P. Chowdhury, B. Crowell, P. J. Ennis, Ch. Winter, T. Drake, A. Galindo-Uribarri, G. Zwartz, H. R. Andrews, G. C. Ball, D. Radford, D. Ward, and V. P. Janzen, Phys. Rev. Lett. 66, 3121 (1991).

[18] E. Erba, U. Facchini, and E. Saetta-Menichella, Nuovo Cimento 22, 1237 (1961).

[19] H. Baba, Nucl. Phys. A159, 625 (1970).

[20] G. Shanmugam and V. Devanathan, Phys. Scr. 24, 17 (1981); 25, 607 (1982).

[21] J. M. Eisenberg and W. Greiner, Microscopic Theory of the Nucleus (North-Holland, New York, 1976), p. 399.

[22] G. Shanmugam, P. R. Subramanian, M. Rajasekaran, and V. Devanathan, in Nuclear Interactions, Vol. 92 of Lecture Notes in Physics, edited by B. A. Robson (Springer, Berlin,

1979), p. 433.

[23] M. Diebel, D. Glas, U. Mosel, and H. Chandra, Nucl. Phys. **A333**, 253 (1980).

[24] J. R. Nix, Annu. Rev. Nucl. Sci. **22**, 65 (1972).

[25] C. Bloch, in *Proceedings of the Statistical Properties of Nuclei,* edited by J. B. Garg (Plenum, New York, 1977), pp.

379 and 403; Phys. Rev. **93**, 1094 (1954).

[26] C. Ngo, in *Proceedings of the Mikolajki Summer School of Nuclear Physics—Heavy Ions and Nuclear Structure,* Poland, 1981, edited by B. Sikora and Z. Wilhelmi (Harwood Academic, New York, 1981), Vol. 5, p. 81.